Insights into noise modulation in oligomerization systems of increasing complexity

Fabrizio Pucci* and Marianne Rooman†

Department of BioModeling, BioInformatics & BioProcesses, Université Libre de Bruxelles, Roosevelt Avenue 50, B-1050 Brussels, Belgium and Department of Theoretical Physics, Université Libre de Bruxelles, Triumph Boulevard, B-1050 Brussels, Belgium

(Received 3 August 2017; revised manuscript received 26 March 2018; published 26 July 2018)

Understanding under which conditions the increase of systems complexity is evolutionarily advantageous, and how this trend is related to the modulation of the intrinsic noise, are fascinating issues of utmost importance for synthetic and systems biology. To get insights into these matters, we analyzed a series of chemical reaction networks with different topologies and complexity, described by mass-action kinetics. We showed, analytically and numerically, that the global level of fluctuations at the steady state, measured by the sum over all species of the Fano factors of the number of molecules, is directly related to the network's deficiency. For zero-deficiency systems, this sum is constant and equal to the rank of the network. For higher deficiencies, additional terms appear in the Fano factor sum, which are proportional to the net reaction fluxes between the molecular complexes. We showed that the system's global intrinsic noise is reduced when all fluxes flow from lower to higher degree oligomers, or equivalently, towards the species of higher complexity, whereas it is amplified when the fluxes are directed towards lower complexity species.

DOI: 10.1103/PhysRevE.98.012137

I. INTRODUCTION

Fluctuations play a major role in the dynamics of a large variety of complex biological processes. To properly describe the stochastic and heterogeneous nature of systems such as the transcriptional machinery [1] or cell differentiation processes [2], stochastic modeling approaches are indispensable [3]. For example, intensive efforts have been devoted in the last decade to the characterization of stochasticity in chemical reaction networks (CRNs) by studying the propagation of fluctuations through the networks [4,5] or by analyzing the relation between thermodynamic properties and noise levels [6,7]. However, the full understanding of the stochastic properties of biomolecular networks remains an intricate goal that is far from being met.

A challenging open question concerns the relationship between the complexity of biological systems and the modulation of the intrinsic noise. At first glance, the evolutionary pressure, which led from unicellular organisms to higher eukaryotes, tends to favor both complexity increase and noise reduction; however, for particular processes such cell differentiation the converse seems to happen. These opposite behaviors are also supported by modeling investigations, which showed that the increase of system complexity is associated to a decrease of the noise level for some systems [8], whereas other complex processes are noise-driven [9]; for still other systems, the intrinsic noise can be either increased or decreased according to the parameter values of the model [10].

The lack of a general understanding is due to the fact that CRNs describing biological systems are usually large and complex and therefore complicated to model mathematically, whether analytically due to the intricacy of equations or via stochastic simulations because the parameter space becomes rapidly too large to be tractable. Hence, only toy models can be realistically analyzed.

In view of deepening our knowledge about noise modulation in stochastic CRNs, we thoroughly analyzed model systems with different degrees of complexity and explored analytically and numerically their dynamical behavior using the Itō stochastic differential equation formalism. We obtained general relations between some characteristics of the CRNs and the noise levels evaluated by the Fano factors of the biochemical species involved. We conjectured the validity of these relations for general classes of CRNs.

II. STOCHASTIC CRNS

Systems of interacting biological molecules are mathematically represented by chemical reaction networks $[\mathcal{S}, \mathcal{C}, \mathcal{R}]$ consisting of sets of chemical species $\mathcal{S}$, elementary reactions $\mathcal{R}$, and complexes $\mathcal{C}$ defined as the input or output of an individual reaction [11]. For example, the CRN $2U_1 \leftrightarrow U_2 \leftrightarrow U_3 + U_1$ has $\mathcal{S} = \{U_1, U_2, U_3\}$, $\mathcal{C} = \{2U_1, U_2, U_3 + U_1\}$, and $\mathcal{R}$ comprises the four reactions indicated by arrows.

Each complex is associated with a vector $\in \mathbb{R}^{\mathrm{card}(\mathcal{S})}$ whose entries are the stoichiometric coefficients of the species in the complex. In the case of open systems, the environment (denoted by $\varnothing$) is considered as a complex in which all species have a vanishing stoichiometric coefficient. Each reaction j in the network is associated with a vector $k_{ij} \in \mathbb{R}^{\mathrm{card}(\mathcal{S})}$ obtained by subtracting the vector of the reactant complex from that of the product. The number of linearly independent reaction vectors is by definition the rank $\mathcal{X}$.

An important parameter that characterizes the CRN is the deficiency [11,12], defined as $\delta = \mathrm{card}(\mathcal{C}) - \mathcal{L} - \mathcal{X}$ where $\mathcal{L}$ is the number of linkage classes or, equivalently, the number of connected network components. In the above example, we

*fapucci@ulb.ac.be
†mrooman@ulb.ac.be

have card($\mathcal{C}$) = 3, $\mathcal{L}$ = 1, and $\mathcal{X}$= 2, and thus the system has zero deficiency.

The dynamical behavior of a CRN can be described by the chemical Langevin equation in the Itō formalism [13]:

$$\frac{dU_i(t)}{dt} = \sum_{j=1}^{\mathrm{card}(\mathcal{R})} k_{ij} a_j(\mathbf{U}(t)) + \sum_{j=1}^{\mathrm{card}(\mathcal{R})} k_{ij} \sqrt{a_j(\mathbf{U}(t))}\, dW^j(t), \qquad (1)$$

where $U_i(t)$ is the number of molecules of species i at time t, $a_j(\mathbf{U}(t))$ is the rate of reaction j, and $W^j(t)$'s are independent Wiener processes. This system of equations describes the temporal evolution of $\mathbf{U}(t)$ and its conditioned probability density function obeys the associated Fokker-Planck equation. It has also been demonstrated to be equivalent to the master equation formalism for sufficiently large numbers of molecules [13–15].

CRNs are said to be complex balanced [11,12] if, for each complex y and each steady state, the sum of the mean reaction rates for the reactions $r \subset \mathcal{R}$ for which y is a reactant complex is equal to the sum of the mean reaction rates for $r' \subset \mathcal{R}$ for which y is a product complex. Detailed balanced CRNs are a subclass of complex balanced systems for which this relation holds separately for each pair of forward and inverse reactions linking two complexes. Detailed balanced steady states correspond to thermodynamic equilibrium states, while the others are nonequilibrium steady states (NESS).

CRNs are also characterized by their reversibility properties. They are said to be reversible if the existence of a reaction that transforms one complex into another implies the existence of the reverse reaction. They are weakly reversible if the existence of a reaction path from complex one to complex two implies the existence of a path from complex two to complex one.

An important result in CRN theory known as the zero deficiency theorem [12] shows that CRNs are complex balanced *if and only if* they are of deficiency zero and weakly reversible. For higher deficiency CRNs, the value of δ corresponds to the number of independent conditions on the rate constants that have to be satisfied in order for the system to be complex balanced. In a certain sense, δ measures the "distance" of the network from complex balancing.

III. MODEL SYSTEMS

We studied three types of weakly reversible CRNs, depicted in Fig. 1 and characterized by different deficiency values (see figure legend). The simplest one [Fig. 1(a)] is defined by the reaction chain:

$$n\ \mathrm{X} \rightleftharpoons \mathrm{Y} \rightleftharpoons \varnothing \rightleftharpoons \mathrm{X}. \qquad (2)$$

It represents, for example, the assembly of monomeric molecules X into homo-oligomers Y, where $n \in \mathbb{N}_{>0}$ indicates the number of monomers in each oligomer. When $n = 1$, this CRN represents the interconversion between two states of the same molecule (e.g., activated or not) or between two localizations (e.g., intra- or extracellular). Both species are linked to the environment.

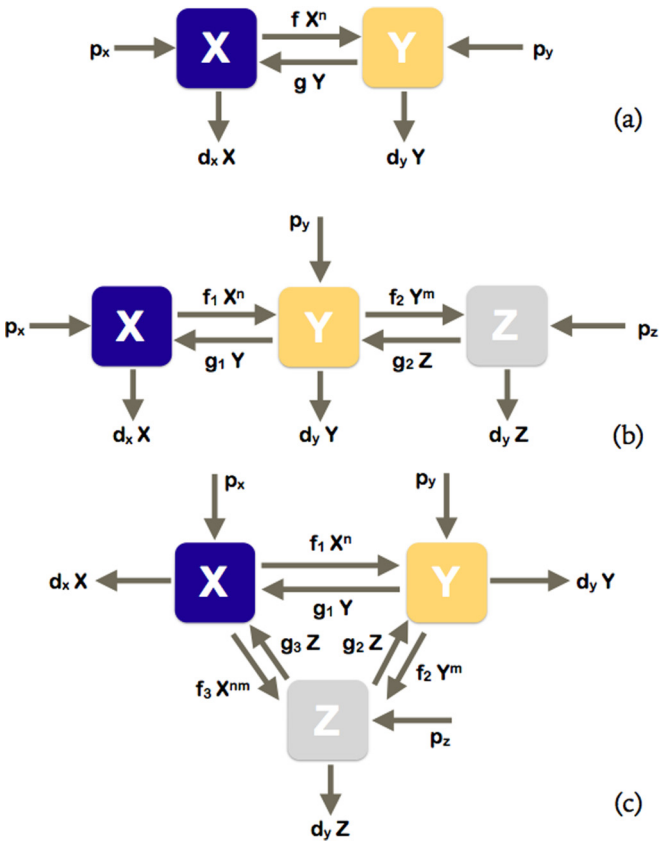

FIG. 1. Schematic picture of the reaction networks analyzed in this letter. (a) CRN of Eq. (2), with $\delta \leqslant 1$ according to the parameter values; (b) CRN of Eq. (3), with $\delta \leqslant 2$; (c) CRN of Eq. (4), with $\delta \leqslant 3$.

We also studied more complex CRNs, which model, for instance, biological systems in which a molecular species undergoes a homo-oligomerization process through an intermediate oligomerization step of lower degree [Fig. 1(b)]:

$$\begin{aligned} n\ \mathrm{X} &\rightleftharpoons \mathrm{Y}, \quad m\ \mathrm{Y} \rightleftharpoons \mathrm{Z}, \\ \mathrm{X} &\rightleftharpoons \varnothing, \ \mathrm{Y} \rightleftharpoons \varnothing, \ \mathrm{Z} \rightleftharpoons \varnothing, \end{aligned} \qquad (3)$$

with $n, m \in \mathbb{N}_{>0}$, or in which the homo-oligomerization process occurs with or without an intermediate step [Fig. 1(c)]:

$$\begin{aligned} n\ \mathrm{X} &\rightleftharpoons \mathrm{Y}, \quad m\ \mathrm{Y} \rightleftharpoons \mathrm{Z}, \quad nm\ \mathrm{X} \rightleftharpoons \mathrm{Z}, \\ \mathrm{X} &\rightleftharpoons \varnothing, \ \mathrm{Y} \rightleftharpoons \varnothing, \ \mathrm{Z} \rightleftharpoons \varnothing. \end{aligned} \qquad (4)$$

IV. ITŌ STOCHASTIC MODELING

For describing the CRN of Eq. (2), the general system of Itō stochastic differential equations (SDEs) given in Eq. (1) reduces to

$$\begin{aligned} dX(t) &= dP_x(t) - dD_x(t) - n\,(dF(t) - dG(t)), \\ dY(t) &= dP_y(t) - dD_y(t) + dF(t) - dG(t), \end{aligned} \qquad (5)$$

where $X(t)$ and $Y(t)$ are the numbers of molecules of species X and Y, $dP_x(t)$ and $dP_y(t)$ the associated production terms,

$dD_x(t)$ and $dD_y(t)$ the degradation terms, and $dF(t)$ and $dG(t)$ the interconversion terms. These terms can be expressed as

$$\begin{aligned} dP_x(t) &= p_x dt + \sqrt{p_x}\, dW^{p_x}(t), \\ dD_x(t) &= d_x X(t) dt + \sqrt{d_x X(t)}\, dW^{d_x}(t), \\ dP_y(t) &= p_y dt + \sqrt{p_y}\, dW^{p_y}(t), \\ dD_y(t) &= d_y Y(t) dt + \sqrt{d_y Y(t)}\, dW^{d_y}(t), \\ dF(t) &= f X(t)^{(n)} dt + \sqrt{f X(t)^{(n)}}\, dW^{f}(t), \\ dG(t) &= g Y(t) dt + \sqrt{g Y(t)}\, dW^{g}(t), \end{aligned} \tag{6}$$

where $p_x, d_x, p_y, d_y, f, g \in \mathbb{R}_{\geqslant 0}$ are the parameters of the model, and $X^{(n)} \equiv X(X-1)...(X-n+1)$ which reduces to $X^{(n)} \approx X^n$ for large numbers of molecules.

The production rates p_x and p_y are considered as constant, the degradation rates $d_x X(t)$ and $d_y Y(t)$ are proportional to the number of molecules, while the interconversion rates $f X(t)^{(n)}$ and $gY(t)$ follow a mass-action kinetic scheme and are proportional to the product of the concentrations of the reactants raised to powers that are equal to their stoichiometric coefficients. The Wiener processes of the six reactions, $W^{p_x}(t)$, $W^{d_x}(t)$, $W^{p_y}(t)$, $W^{p_x}(t)$, $W^{d_x}(t)$, $W^{f}(t)$, and $W^{g}(t)$, are all independent [16].

The next step consists of approximating these continuous-time SDEs by discrete-time SDEs. Therefore, we divided the time interval $[0, T]$ into Ξ equal-length intervals $0 = t_0 < \ldots < t_\Xi = T$, with $t_\tau = \tau \Delta t$ and $\Delta t = T/\Xi$. Using the Euler-Maruyama discretization scheme [17], the discrete-time SDEs read as

$$\begin{aligned} X_{\tau+1} &= X_\tau + (p_x - d_x X_\tau)\Delta t \\ &\quad + \sqrt{p_x}\, \Delta W_\tau^{p_x} - \sqrt{d_x X_\tau}\, \Delta W_\tau^{d_x} \\ &\quad - n\left(f X_\tau^{(n)} - g Y_\tau\right)\Delta t \\ &\quad - n\left(\sqrt{f X_\tau^{(n)}}\, \Delta W_\tau^{f} - \sqrt{g Y_\tau}\, \Delta W_\tau^{g}\right), \\ Y_{\tau+1} &= Y_\tau + (p_y - d_y Y_\tau)\Delta t \\ &\quad + \sqrt{p_y}\, \Delta W_\tau^{p_y} - \sqrt{d_y Y_\tau}\, \Delta W_\tau^{d_y} \\ &\quad + \left(f X_\tau^{(n)} - g Y_\tau\right)\Delta t \\ &\quad + \left(\sqrt{f X_\tau^{(n)}}\, \Delta W_\tau^{f} - \sqrt{g Y_\tau}\, \Delta W_\tau^{g}\right). \end{aligned} \tag{7}$$

The independent Wiener processes satisfy $W_\tau = W(t_\tau)$ and $\Delta W_\tau = W_{\tau+1} - W_\tau$, so that $W_0 = 0$, $\mathbf{E}[\Delta W_\tau] = 0$ and $\mathbf{Var}[\Delta W_\tau] = \Delta t$. This system converges towards a steady state in the long-time limit, obtained by first taking the limit $T = \Xi \Delta t \to \infty$ followed by $\Delta t \to 0$. In the following, we represent the values of the variables at the steady state without subscript, e.g., $X_\tau \to X$.

We computed and equated the mean of the left and right sides of Eq. (7), as well as the mean of their squares and of their product, and then take the steady-state limit. Requiring that the leading Δt contribution vanishes in each equation, we obtained five independent algebraic equations that link the moments $\mathbf{E}[X]$, $\mathbf{E}[Y]$, $\mathbf{Var}[X]$, $\mathbf{Var}[Y]$, and $\mathbf{Cov}[X, Y]$ to the model parameters and to some higher order moments $\mathbf{Cov}[X, X^{(n)}]$, $\mathbf{Cov}[Y, X^{(n)}]$, and $\mathbf{E}[X^{(n)}]$

$$\begin{aligned} &\frac{1}{n}(p_x - d_x \mathbf{E}[X]) \\ &\quad = f\mathbf{E}[X^{(n)}] - g\mathbf{E}[Y] = -p_y + d_y \mathbf{E}[Y], \\ &2\,\mathbf{Cov}[X, d_x X + nf X^{(n)} - ngY] \\ &\quad = p_x + d_x \mathbf{E}[X] + n^2 f \mathbf{E}[X^{(n)}] + n^2 g \mathbf{E}[Y], \\ &2\,\mathbf{Cov}[Y, d_y Y + gY - f X^{(n)}] \\ &\quad = p_y + d_y \mathbf{E}[Y] + f\mathbf{E}[X^{(n)}] + g\mathbf{E}[Y], \\ &\mathbf{Cov}[X, d_y Y + gY - f X^{(n)}] + \mathbf{Cov}[Y, d_x X + nf X^{(n)} \\ &\qquad - ngY] = -nf\mathbf{E}[X^{(n)}] - ng\mathbf{E}[Y]. \end{aligned} \tag{8}$$

When $n > 1$, the number of moments is larger than the number of algebraic equations, so we cannot solve this system completely. For this, we need to approximate the higher order moments in terms of the lower order ones, i.e., in terms of the mean, variance, and covariance of X and Y. We used for that purpose the moment closure approximation (MCA), which has been developed to achieve a closed form for sets of coupled stochastic differential equations, which otherwise would be intractable [18–20]. There are several MCA schemes, among which the normal MCA that seems in general to perform better than the others [19,21]. This MCA scheme yields the following relations connecting higher to lower order moments:

$$\begin{aligned} \mathbf{Cov}[X, X^n] &\approx n\, \mathbf{E}[X^n] \frac{\mathbf{Var}[X]}{\mathbf{E}[X]}, \\ \mathbf{Cov}[Y, X^n] &\approx n\, \mathbf{E}[X^n] \frac{\mathbf{Cov}[X, Y]}{\mathbf{E}[X]}. \end{aligned} \tag{9}$$

These approximations are valid if $\mathbf{Var}[X] \ll \mathbf{E}[X]^2$ and $\mathbf{Var}[Y] \ll \mathbf{E}[Y]^2$. In what follows, we also made the approximation $\mathbf{E}[X^{(n)}] \approx \mathbf{E}[X^n]$, which is valid for $\mathbf{E}[X] \gg 1$.

Even though the Itō SDE formalism involves some approximations that the master equation formalism does not, it has also substantial advantages. The first is that both the analytical and numerical results can be obtained more efficiently [14,22], an important point since our systems are complex and the stochastic simulations suffer from poor convergence properties. The second advantage is that Itō SDEs allow improved conceptual understanding of the noise modulation since the drift and random fluctuating contributions to each of the reactions can be more easily identified [14].

V. INTRINSIC NOISE

A central parameter that quantifies the role of fluctuations in biochemical systems is the Fano factor $\mathbf{F}(U(t))$, defined as the ratio between the variance of a stochastic variable $U(t)$ to its mean:

$$\mathbf{F}(U(t)) = \mathbf{Var}[U(t)]/\mathbf{E}[U(t)]. \tag{10}$$

If the variable follows a Poisson distribution, its Fano factor $\mathbf{F}$ is equal to one. When $\mathbf{F}$ is larger than one, the fluctuations affect more strongly the variable concentration and the distribution is called super-Poissonian. The distribution is sub-Poissonian when $\mathbf{F} < 1$.

To analyze the role of the fluctuations in the different types of CRNs depicted in Fig. 1, we computed the sum of the Fano factors of all species at the steady state as a function of the system's parameters. This sum represents the global noise level of the system.

For the CRN of Fig. 1(a), the Fano factors are obtained from the system of SDEs of Eq. (5), whose solution is given by Eq. (8) with the MCA approximations of Eq. (9). For the CRNs connecting three species, depicted in Figs. 1(b) and 1(c), the SDEs are easily generalized and solved according to the same procedure. The details of all the computations and the analytical results are given in the Supplemental Material [23].

A. Deficiency zero

Several of the CRNs depicted in Fig. 1 have zero deficiency. A first class consists of the CRNs of Figs. 1(a) and 1(b) for which all production and degradation parameters vanish, or for which they vanish for all species except one. These CRNs are detailed balanced since they admit detailed balanced steady states for all (other) parameter values. Another class of $\delta = 0$ systems is characterized by $n = 1$ in Fig. 1(a) and $n = 1 = m$ in Figs. 1(b) and 1(c). These networks are complex balanced but not detailed balanced.

For all these systems, we found analytically that the sum of the Fano factors of all species is equal to the rank at the steady state:

$$\sum_{i=1}^{\mathrm{card}(\mathcal{S})} \mathbf{F}_i = \mathcal{X}. \tag{11}$$

It can be checked that *all CRNs with deficiency zero satisfy this simple relation*. This result is directly related to the fact that, for $\delta = 0$ CRNs, the steady-state probability distribution of the number of molecules is a product of Poisson distributions, or a multinomial distribution in the case some conservation laws hold and thus the state space is reduced, as, for example, in closed systems where the number of molecules is conserved [24,25].

B. Higher deficiency

For systems with deficiency larger than zero, the situation becomes more complicated due to the nonzero correlations between the chemical species in the steady state. We started considering the $\delta = 1$ homo-oligomerization CRN shown in Fig. 1(a), with $n > 1$ and the two species X and Y linked to the environment. Their dynamical behavior is modeled by Eqs. (5) and (6) and the steady-state solutions are obtained from Eqs. (8) and (9).

In this case, the mean internal flux Ψ that flows between the two species X and Y,

$$\Psi = f\,\mathbf{E}[X^n] - g\,\mathbf{E}[Y], \tag{12}$$

is generally nonzero, and proportional to the mean fluxes that involve exchanges with the environment. In terms of Ψ and the system's rank $\mathcal{X}$ (here equal to two), we found analytically that the sum of the Fano factors of all species at the steady state

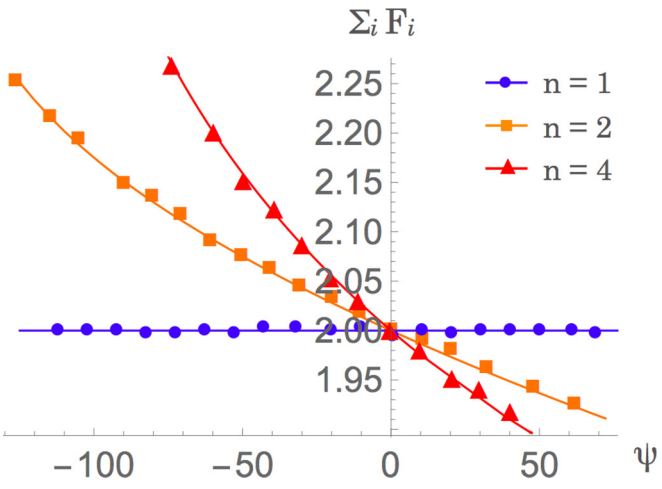

FIG. 2. Sum of Fano factors of the two species X and Y of the CRN of Fig. 1(a), as a function of the mean flux Ψ, for different values of the parameters n and f; all other parameters are kept fixed: $p_x = p_y = 200$, $d_x = d_y = 0.001$, and $g = 0.002$. The analytical solutions are indicated with lines and the solutions from stochastic simulations with dots, squares or triangles according to the value of n.

satisfies the relation,

$$\sum_{i=1}^{\mathrm{card}(\mathcal{S})} \mathbf{F}_i = \mathcal{X} - \alpha\,(n-1)\,\Psi, \tag{13}$$

where α is a *positive* function,

$$\alpha = \frac{n}{2\mathbf{E}(Y)}\,\frac{A}{B}, \tag{14}$$

with

$$\begin{aligned} A &= n^2 f^2 \mathbf{E}[X^n]^2 + n^2 f d_y \mathbf{E}[Y]\mathbf{E}[X^n] \\ &\quad + (g + d_y)(g + d_x + d_y)\mathbf{E}[X]\mathbf{E}[Y], \\ B &= n^4 f^2 d_y \mathbf{E}[X^n]^2 + d_x(g + d_y)(g + d_x + d_y)\mathbf{E}[X]^2 \\ &\quad + n^2 f(d_x(g + d_y) + d_y(g + d_x + d_y))\mathbf{E}[X]\mathbf{E}[X^n]. \end{aligned}$$

Note that $\mathbf{E}[X^n]$, $\mathbf{E}[X]$, and $\mathbf{E}[Y]$ can be expressed in terms of the system's parameters $(p_x, p_y, d_x, d_y, f, g)$ for each value of n, using Eqs. (8) and (9).

Equation (13) reduces to Eq. (11) when $n = 1$ in which case $\delta = 0$, or when $\Psi = 0$ in which case the steady state (but not necessarily the system) is detailed balanced. The Fano factor sum as a function of Ψ is plotted in Fig. 2, for different values of the parameters n and f.

According to Eq. (13), the global intrinsic noise level is reduced when the mean flux Ψ is positive, thus when it is directed towards the oligomer Y. In contrast, it is amplified when Ψ is directed towards the monomer X. Interestingly, the larger the degree—or complexity level—of the oligomer, the larger the reduction or amplification effect. Indeed, the proportionality coefficient between the Fano factor sum and the flux increases in absolute value with n, as illustrated in Fig. 2.

To estimate the intrinsic noise in higher deficiency systems, we considered the $\delta = 2$ CRN of Fig. 1(b). It has two fluxes

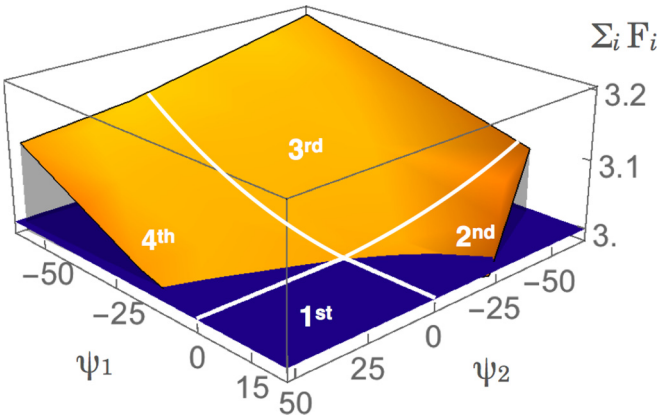

FIG. 3. Sum of Fano factors of the three species X, Y, and Z as a function of the two (independent) mean fluxes Ψ_1 and Ψ_2, for different values of parameters f_1 and f_2, for the CRNs depicted in Fig. 1(b) with $n = m = 2$; all other parameters are kept fixed: $p_x = p_y = p_z = 100$, $d_x = d_y = d_z = 0.001$, $g_1 = g_2 = 0.01$. The dark-color surface is $\sum_i \mathbf{F}_i = 3$, while the light-color surface is obtained by solving the SDE system. In quadrant I (III), where the fluxes are both negative (positive), there is an increase (decrease) of the global noise. In quadrants II and IV, both scenarios are possible according to the models' parameters.

that are in general nonzero and flow between pairs of species:

$$\Psi_1 = f_1\,\mathbf{E}[X^n] - g_1\,\mathbf{E}[Y],$$
$$\Psi_2 = f_2\,\mathbf{E}[Y^m] - g_2\,\mathbf{E}[Z]. \tag{15}$$

The fluxes that link the species to the environment are linear combinations of these two fluxes. We also considered the $\delta = 3$ CRN of Fig. 1(c). This system has three internal fluxes, the two given by Eq. (15) and

$$\Psi_3 = f_3\,\mathbf{E}[X^{nm}] - g_3\,\mathbf{E}[Z]. \tag{16}$$

We showed analytically for all parameter values, and checked numerically for some of them, that the global intrinsic noise at the steady state satisfies the relation,

$$\sum_{i=1}^{\mathrm{card}(\mathcal{S})} \mathbf{F}_i = \mathcal{X} - \sum_{\ell=1}^{N_\Psi} \alpha_\ell K_\ell\, \Psi_\ell, \tag{17}$$

where all α_ℓ's are *positive* functions of the parameters and the sum is over the N_Ψ internal mean fluxes, i.e., $N_\Psi = 2$ and 3 for the systems of Figs. 1(b) and 1(c), respectively. The K_ℓ coefficient is defined in terms of the reaction vectors, $K_\ell = \frac{1}{2}\sum_i^{\mathrm{card}(\mathcal{S})}(k_{i\ell^-} - k_{i\ell^+})$ where ℓ^+ and $\ell^- \in \mathcal{R}$ represent the forward and backward reactions associated with the flux Ψ_ℓ. Here K_ℓ is equal to $(n-1)$, $(m-1)$, and $(n\,m-1)$ for $\ell = 1, 2, 3$, and the rank is $\mathcal{X} = 3$.

We conjecture that *Eq. (17) remains valid for generic homo-oligomerization CRNs*, where the sum is over the N_Ψ internal fluxes defined as functions of forward and backward reaction rates as $\Psi_\ell = \mathbf{E}[a_{\ell^+} - a_{\ell^-}]$. Note that the internal fluxes for which the stoichiometries of the reactant and product complexes are equal (which implies $k_{i\ell^-} = 0 = k_{i\ell^+}$) do not contribute to this equation since K_ℓ is vanishing.

Equation (17) shows that when all the fluxes flow from the species of lower complexity (defined in terms of the oligomerization degree) to the species of higher complexity, the global intrinsic noise level is reduced. In contrast, when the fluxes are directed towards the lower complexity species, it is amplified. When the fluxes do not all have the same sign, there starts to be a competition between them and whether the global intrinsic noise is amplified or reduced depends on the relative weight of the $\alpha_\ell \geqslant 0$ coefficients. This is pictorially shown in Fig. 3 for the model system of Fig. 1(b).

VI. CONCLUSION

In this article, we demonstrated that the sum of the Fano factors of all chemical species involved in a CRN depend crucially on the value of the deficiency. For all weakly reversible CRNs with $\delta = 0$, the Fano factor sum is always constant and equal to the rank of the system independently of the model's parameters. From a physical point of view, this can be related to the fact that, for $\delta = 0$ CRNs, the entropy production rate of the stochastic model equals that of the corresponding deterministic system, where correlations between chemical species vanish [6].

For higher deficiency systems, in which the different species are correlated, additional terms appear which are proportional to the fluxes between the complexes and the associated stoichiometric coefficients. If all fluxes flow in the direction of higher complexity, a global reduction of the fluctuations is observed, while an amplification occurs when the fluxes are directed towards lower complexity.

To get insights into the biological meaning of our results, consider the system composed of monomeric proteins that undergo a homo-oligomerization process. In this case [Fig. 1(a) with $p_y = 0$] the mean flux is directed towards higher complexity and thus the sum of Fano factors is always smaller than or equal to the rank, which signals global noise reduction. In contrast, for systems modeling the chemical hydrolysis of cellulose into monomeric sugars, where instead $p_x = 0$ and the flux is directed towards the lowest complexity species, we always have global noise amplification.

Several points remain to be addressed to get a full picture of noise modulation in biological systems. The analysis of the Fano factors of each individual chemical species is left for upcoming papers [26,27]. Our results also need to be extended to more complex systems as well as to more general kinetic schemes [28,29]. Last but not least, a clear interpretation of our results in terms of entropy production rates will contribute to deepen our physical understanding of these systems [6,7].

ACKNOWLEDGMENTS

F.P. and M.R. acknowledge the Belgian Fund for Scientific Research (F.R.S.-FNRS) for support.

[1] M. Elowitz, A. Levine, E. Siggia, and P. Swain, Stochastic gene expression in a single cell, Science **297**, 1183 (2002).

[2] G. Balazsi, A. van Oudenaarden, and J. J. Collins, Cellular decision-making and biological noise: From microbes to mammals, Cell **144**, 910 (2011).

[3] D. J. Wilkinson, Stochastic modeling for quantitative description of heterogeneous biological systems, Nat. Rev. Genet. **10**, 122 (2009).

[4] D. F. Anderson, J. C. Mattingly, H. F. Nijhout, and M. C. Ree, Propagation of fluctuations in biochemical systems, I: Linear SSC networks, Bull. Math. Biol. **69**, 1791 (2007).

[5] D. F. Anderson and J. C. Mattingly, Propagation of fluctuations in biochemical systems, II: Nonlinear chains, IET Syst. Biol. **1**, 313 (2007).

[6] M. Polettini, A. Wachtel, and M. Esposito, Dissipation in noisy chemical networks: The role of deficiency, J. Chem. Phys. **143**, 184103 (2015).

[7] R. Rao and M. Esposito, Nonequilibrium Thermodynamics of Chemical Reaction Networks: Wisdom from Stochastic Thermodynamics, Phys. Rev. X **6**, 041064 (2016).

[8] L. Cardelli, A. Csikász-Nagy, N. Dalchau, M. Tribastone, and M. Tschaikowski, Noise reduction in complex biological switches, Scientific Reports **6**, 20214 (2016).

[9] M. Hoffmann, H. H. Chang, S. Huang, D. E. Ingber, M. Loeffler, and J. Galle, Noise-driven stem cell and progenitor population dynamics, PLoS ONE **3**, e2922 (2008).

[10] M. Rooman, J. Albert, and M. Duerinckx, Stochastic noise reduction upon complexification: Positively correlated birth-death type systems, J. Theor. Biol. **354**, 113 (2014).

[11] M. Feinberg, Chemical reaction network structure and the stability of complex isothermal reactors. I. The deficiency zero and deficiency one theorems, Chem. Eng. Sci. **42**, 2229 (1987).

[12] F. J. M. Horn, Necessary and sufficient conditions for complex balancing in chemical kinetics, Arch. Rat. Mech. Anal. **49**, 172 (1972).

[13] D. T. Gillespie, The chemical Langevin equation, J. Chem. Phys. **113**, 297 (2000).

[14] D. T. Gillespie, The chemical langevin and fokker-planck equations for the reversible isomerization reaction, J. Phys. Chem. A **106**, 5063 (2002).

[15] D. Schnoerr, G. Sanguinetti, and R. Grima, The complex chemical Langevin equation, J. Chem. Phys. **141**, 024103 (2014).

[16] E. Allen, *Modeling with Itō Stochastic Differential Equations* (Springer, Amsterdam, 2007).

[17] P. E. Kloeden and E. Platen, *Numerical Solution of Stochastic Differential Equations* (Springer, Berlin, 1992).

[18] C. Kuehn, in *Moment Closure – A Brief Review, Control of Self-Organizing Complex Systems*, edited by E. Schöll, S. Klapp, and P. Hövel (Springer, Berlin, 2016), pp. 253–271.

[19] R. Grima, A study of the accuracy of moment-closure approximations for stochastic chemical kinetics, J. Chem. Phys. **136**, 154105 (2012).

[20] D. Schnoerr, G. Sanguinetti, and R. Grima, Comparison of different moment-closure approximations for stochastic chemical kinetics, J. Chem. Phys. **143**, 185101 (2015).

[21] D. Schnoerr, G. Sanguinetti, and R. Grima, Validity conditions for moment closure approximations in stochastic chemical kinetics, J. Chem. Phys. **141**, 084103 (2014).

[22] D. Schnoerr, G. Sanguinetti, and R. Grima, Approximation and inference methods for stochastic biochemical kinetics – a tutorial review, J. Phys. A: Math. Theor. **50**, 093001 (2017).

[23] See Supplemental Material at http://link.aps.org/supplemental/10.1103/PhysRevE.98.012137 for the details of all the computations and the analytical results for the SDE systems that are analyzed in the paper.

[24] D. F. Anderson, G. Craciun, and T. G. Kurtz, Product-form stationary distributions for deficiency zero chemical reaction networks, Bull. Math. Biol. **72**, 1947 (2010).

[25] D. K. Lubensky, Equilibriumlike behavior in chemical reaction networks far from equilibrium, Phys. Rev. E **81**, 060102 (2010).

[26] F. Pucci and M. Rooman, Deciphering noise amplification and reduction in open chemical reaction networks, arXiv:1801.08515 [q-bio.MN].

[27] M. Rooman and F. Pucci, Intrinsic noise modulation in closed oligomerization-type systems, IFAC-PapersOnLine **51**, 649 (2018).

[28] A. C. Barato and U. Seifert, Universal bound on the Fano factor on enzyme kinetics, J. Phys. Chem. B **119**, 6555 (2015).

[29] D. F. Anderson and S. L. Cotter, Product-form stationary distributions for deficiency zero networks with non-mass action kinetics, Bull. Math. Biol. **78**, 2390 (2016).